Numerical Analysis of Fractured Process in Locomotive Steel Wheels

J. Alizadeh K., R. S. Ashofteh, A. Asadi Lari

Abstract—Railway vehicle wheels are designed to operate in harsh environments and to withstand high hydrostatic contact pressures. This situation may result in critical circumstances, in particular wheel breakage. This paper presents a time history of a series of broken wheels during a time interval [2007-2008] belongs to locomotive fleet on Iranian Railways. Such fractures in locomotive wheels never reported before. Due to the importance of this issue, a research study has been launched to find the potential reasons of this problem. The authors introduce a FEM model to indicate how and where the wheels could have been affected during their operation. Then, the modeling results are presented and discussed in detail.

Keywords—Crack, fatigue, FE analysis, wheel.

I. INTRODUCTION

RAILWAY wheels are deployed to carry loads and guide rail vehicles on the track. It is very important to design and manufacture steel wheels to ensure their safe operation. So, there are a variety of general and specific railway standards to determine material properties, process of manufacturing and inspection tests before the delivery of the wheels to the customers. However, wheels might be with a series of surface and subsurface defects mostly due to operational aspects, and rarely due to initial inclusions inside the wheel material. The authors of this paper present their findings during a research study focused on a fractured wheel of freight locomotive. This is conducted from different viewpoints to find out its possible failure reasons. It was initially assumed that increasing forces within the contact patch could have governed the bearing stress of the wheel material. The surface and subsurface of the wheel were then subjected to crack propagation process, though possibly with various mechanisms. As a result, a finite element model was developed to for stress analysis. It was found that the possible cause of wheel fracture was likely initiation of cracks followed by their propagation from the wheel subsurface region. It will be continued then to compare and verify the numerical findings with extensive experimental work.

II. INFLUENCING PARAMETERS

According to the literature [1], three influencing parameters

J. Alizadeh K. is with the Faculty of Mechanical Engineering, Islamic Azad University, Parand Branch, Iran (corresponding author, phone: 98-912-4583704; e-mail: j_alizadeh@dena.kntu.ac.ir).

R. S. Ashofteh, is with the Faculty of Mechanical Engineering, Islamic Azad University, Parand Branch, Iran.

A. Asadi Lari is with the Faculty of Mechanical Engineering, Islamic Azad University, Parand Branch, Iran.

in the domain of contact mechanics include material properties, interacting forces and the geometry of contacting bodies. Hence, each of these parameters is described concisely below.

A. Wheel Loading Configurations

Locomotive steel wheels are subjected to a series of normal and tangential forces due to the weight, curving and tractive effort. On the other hand, large braking forces from its contact type, i.e., brake shoes on the wheel tread, and its non-contact type, i.e., auxiliary dynamic braking system could highly affect the wheel surface. Moreover, wheel slip protection system of this specific locomotive, in addition to the application of a new generation of traction motor, i.e., AC type with a higher capability of power transmission, might have enhanced the adhesion coefficient. Hence, such an increased tractive effort could substantially influence material behavior of the wheels.

B. Wheel Material Properties

In order to adapt various large forces within the wheel/rail interface with wheel material properties, the application of a variety of steel wheels have been proposed by the railway regulations. For instance, R1 to R3, and R6 to R9 steel grades for solid wheels (monobloc), and B1 to B7 steel grades for tyred wheels. The former grades are frequently used for motored axles of locomotives, while the latter grades are exclusively employed for non-motored coaches and wagons. Also, a number of these grades have sufficient carbon content to be heat treated to increase their resistance capability.

A variety of pearlitic steel wheels is used in Iranian Railways for motored axle rail vehicles such as 2 trainsets, railbuses and locomotives. Table I represents mechanical properties of those wheels.

C. The Effect of Geometry

Wheel dimensions and profile are significant factors to change dynamic related issues and stress configurations. For instance, wheel diameter can vary the size of the contact patch. Furthermore, any change in the diameter of a locomotive wheel could vary the applied torque within the tread region either in the acceleration or the braking process. Wheel profile could considerably affect dynamic behavior of the wheelsets and the related bogie through the equivalent conicity. Also, the shape, size and location of the contact patch are subjected to the wheel profile, and its lateral displacement and gradual variations. As a result, the profile is usually considered by the researchers in the railway field.

TABLE I
MECHANICAL CHARACTERISTICS FOR A NUMBER OF MONOBLOC STEEL WHEELS [2]

Steel grade	R8T	R9T
Steel condition Heat treatment	Rim-chilled	Rim-chilled
Proof strength (MPa)	-	640
Tensile strength (MPa)	860-980	900-1050
Elongation in 2”	13%	12%
Hardness HB	255-285	262-311
Charpy U impact value	Min 15J	Min 10J

III. TECHNICAL SPECIFICATIONS

The fractured wheels belong to a specific type of locomotives which are mainly employed for freight trains in Iranian network, specifically within southeast region. The bogie configuration of these locomotives is CO-CO, and all axles are equipped with traction motors.

The locomotive wheel profile is a worn profile, which entitled FSDR3 in the technical drawing. The new wheels have 1067mm diameter and 140mm width, and are mostly moved on the UIC60 rails with a 1:20 inclination.

Table II represents a number of vital specifications of locomotive, and wheels [3].

TABLE II
TECHNICAL INFORMATION OF LOCOMOTIVE AND STEEL WHEELS [3]

Items	Specifications
Type of loco	Diesel-electric
Weight (axel load)	150 (25) tonne
Power on the axle	Actual power=650 hp
Max operational speed	110 km/hr
Bogie construction	H-type
Wheel grade	R9T
Wheel profile	FSDR3
Rail profile	UIC60-1:20
Wheel diameter	1067 mm

IV. WHEEL CONTACT SURFACE

A. Common Features and Problems

Wheels are suffered from a set of failure mechanisms, including wheel flat, and wheel burn. Thermal cracks can also be found in the wheel profiles due to excessive braking, when brake shoes on the contact surface are continuously used. In fact, wear is likely an undesirable phenomenon since it causes material removal but, in practice, it can also truncate surface cracks within the contact surface. Although rails are produced, in general, using higher strength steel than wheels and also with greater hardness, both the rails and wheels can be affected by failure mechanisms such as rolling contact fatigue (RCF). On the other hand, the higher wear rate of the wheels within the contact surface has been considered as helpful in preventing the propagation process of the surface and close to subsurface cracks [4].

B. Surface Defects

Rolling contact fatigue which is classified as head checking, shelling and spalling is currently a failure type for steel wheels. Surface cracks are created due to plastic deformation and the ductility property when it becomes exhausted. Depending on the stress amplitude and its either unidirectional or bidirectional condition, various material behavior could be expected as shown in Fig. 1.
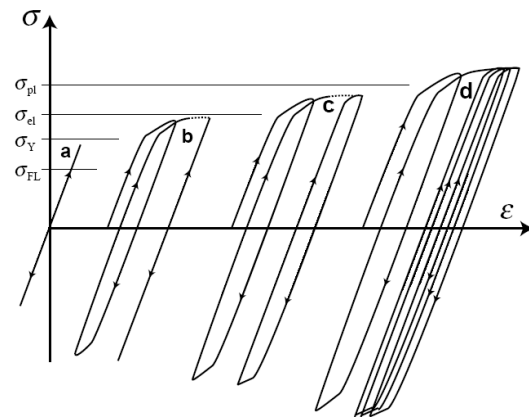

Fig. 1 Material response to a cyclic loading, (a) elastic deformation, (b) elastic shakedown, (c) plastic shakedown, (d) ratcheting [5]

Every loading cycle can increase plastic deformation gradually within the contact surface along the applied tensile load when the stress goes further a given value. As a result, cracks form when fracture strain is reached. The growth of these cracks occurs in the modes II and III. Surface cracks become larger radially towards either the axle or the contact surface which causes material removal, the so called pitting. Furthermore, in specific cases, thermal loading could propagate cracks in radial direction. According to Ekberg and Sotkovszki [6], lubricants cannot affect the growth of wheel surface cracks. Elastic or elasto-plastic modeling could specify whether material properties, loading configuration, and geometry of contact surfaces cause plastic deformation and surface fatigue or not. Such surface fatigue value could then be determined through calculated stresses and strains using a fatigue criterion. A combination of a low cycle multiaxial fatigue criterion and ratcheting failure could successfully predict fatigue in the rail [7].

C. Subsurface Defects

Perhaps subsurface cracks could be categorized as subsurface defects. The most critical fatigue failure within steel wheels is due to subsurface cracks. They tend to be initiated under the surface when adhesion coefficient is about 0.3. Flange contact can also lead to subsurface cracks. The cracks are usually initiated at the depth of 4-20 mm, due to following reasons [7]: (1) strain hardening value is larger at the surface, (2) compression residual stresses due to manufacturing process and wheel operation could prevent fatigue cracks within the surface, (3) any inclusion even at a far depth can cause high local stress. More than 10mm depth, the stress magnitude is infinitesimal, but stress concentration

due to an inclusion could lead to fatigue crack initiation. While it is close to the contact surface, geometry plays vital role. Since cracks propagate under pressure and shear which make a slippage between the mating surfaces of cracks, such inclusions could be removed due to wear. As a result, it is perceived that inclusions become less critical amongst the researchers [7].

The mechanism of subsurface crack growth is shown in Fig. 2. Since plastic deformation within subsurface cracks is low, multiaxial elastic fatigue criteria could be deployed for its modeling.
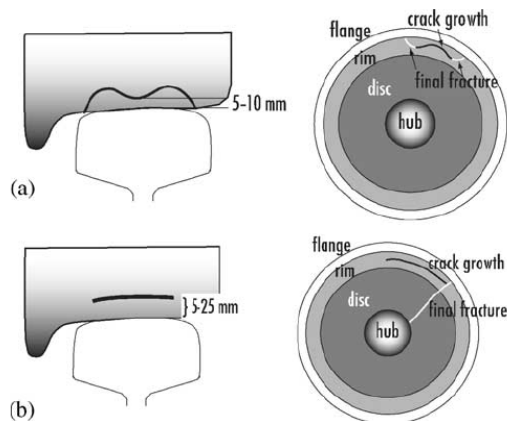
Fig. 2 Typical appearance of subsurface fatigue cracks in steel wheels: (a) shallow initiation, (b) deep initiation at a defect [7]

V. FINITE ELEMENTS ANALYSIS

Ringsberg created a rail F.E.M model representing 120 mm of a track [8]. The distribution of contact pressure and shear stress from wheel/rail contact were applied at a symmetry line on the top surface of the rail model, and it was moved in the rolling direction. The normal contact load distribution was modeled according to the Hertz theory of rolling contact between two elastic non-conforming solids with a smooth and continuous contact surface. Both the wheel and rail were modeled using FEM mesh, and the wheel was then loaded and rotated in the rolling direction on the rail.

Makoto used a wheel and a piece of rail at a F.E.A Model [9]. The wheel and rail models were constructed using eight-node brick elements, and the number of elements in each model is 11418 and 12516 respectively. The wheel shape is the same as that used for Shinkansen train. The rail was modeled as a 60-kg Shinkansen rail and represents 200mm length of a track. The axle was loaded at the node to which the vehicle weight is applied in reality with a concentrated force in the vertical direction.

The rail length equals the length between two sleepers (Approx. 600mm). Fixed boundary conditions were applied by Y. Liu [10] to the full model using 3D element (SOLID 45 in ANSYS). In the contact region a finer mesh was used. All the external loading and boundary conditions of the wheel are applied on the centre of wheel.

A model, namely LocoWheel, was developed in the ABAQUS software tool for this study. The aim of the modeling is stress calculations at the wheel/rail contact zone for analyzing the stresses to find potential location of the crack initiation. A piece of rail with 600mm length (which is the distance between two sleepers), is assumed as a wheel support. A general view of the wheel model which is supported by a piece of rail is shown in Fig. 3. Also, the principle directions of the wheel are schematically shown.
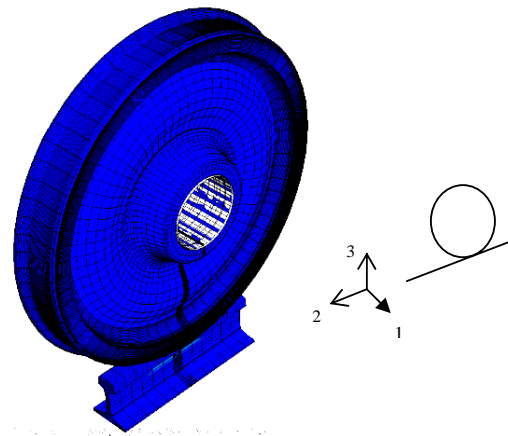

Fig. 3 FE model of wheel and rail

The kind of analysis in the ABAQUS is a Static General Approach. The friction coefficient between wheel and rail is assumed to be 0.35 and directionality isotropic. The next step is to apply the elements to the model. The wheel and rail element shape is in Hexagonal linear solid form and the element type is C3D8R (An 8-node linear brick, hourglass control). It is perceived that the element is involved with the maximum normal stress. To achieve the exact and converged outputs, the contact area was partitionied as the finer meshing. The wheel model has 19530 elements and the rail model has 6692 elements. Fig. 4 shows the contact region in the top view of the wheel, but firstly within the contact surface and also at the subsurface (in a cross section).

The location of the applied load is along the wheel centre vertical axis and 70mm from the back of the wheel flange. Assuming an equal distribution of the locomotive weight, the wheel load is determined as 12.5 tonne. The rail foundation is assumed to be rigid and also restrained. The wheel displacement is fully restricted and is assumed to be free only on the Y direction (the direction of vertical load on the wheel).
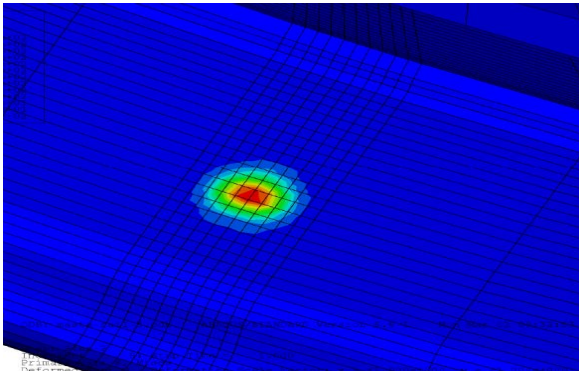
Fig. 4 Top view of the contact area

VI. RESULTS AND DISCUSSION

Every point on the wheel surface experiences fatigue loading due to wheel rotation. In other words, during rotation on the rail within a limited time interval (2%), an applied load to a given point varies to a maximum value and then becomes zero. At the remainder of rotation, the stress field of the point remains zero. In this research study a static analysis was utilized. The gradual loading applied on the wheel was assumed as equal fatigue loading. Therefore, the FEA results have been presented within the given time interval.

Fig. 4 illustrates the Hertz elliptical region within the wheel- rail contact area. The contact patch dimension is varied due to a gradual loading process.

The variation of the semi-elliptical axes due to a gradual loading procedure is shown in Fig. 5.
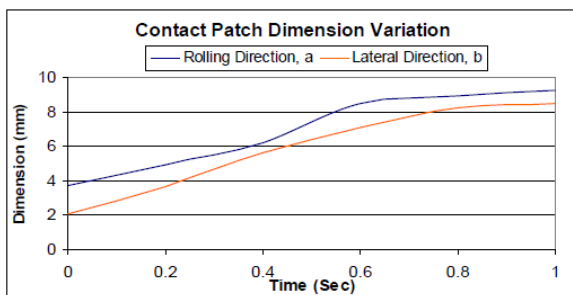

Fig. 5 Semi-elliptical axes variation

Minimum principle stress is illustrated in Fig. 6. It is shown that 2 nodes gained magnitudes beyond 800 MPa, which is greater value than the proof strength of R9T grade, see Table I (note that 4 nodes are in the range 600-800 MPa).
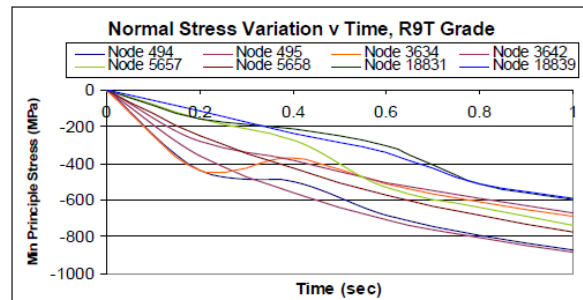

Fig. 6 The variation of normal stress

Fig. 4 illustrates a general view of the contact patch, but the equivalent stress magnitude is shown in Fig. 6. Also, at the end of gradual loading process, i.e., t=1 sec, the node number with maximum normal stress could be obtained.

The wheel surface has been reached the plastic deformation mode at the first contact, when seeing a greater magnitude of normal stress than the proof stress of R9T grade steel as presented in Table I.

As described earlier, plastic deformation mode has priority to crack initiation. As a result, the wheel under investigation is subject to crack initiation even when its material has no any inclusions.

Although it is expected to observe identical max strain during gradual loading, the last node trend shows a rather sharp decline when it was gained a maximum principle strain at 0.8 sec time scale (see Fig. 7).
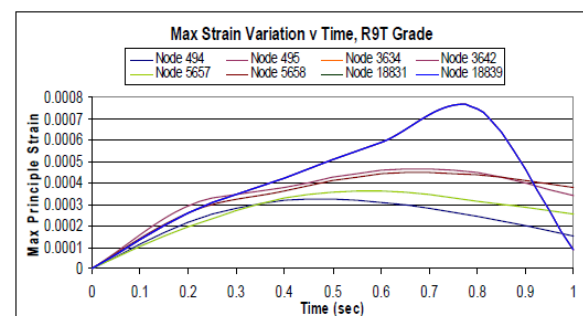

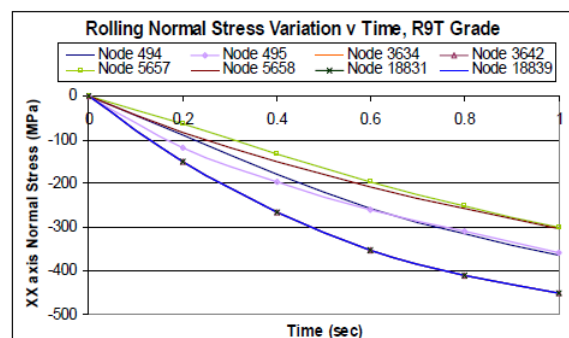Fig. 7 The variation of maximum principle strain

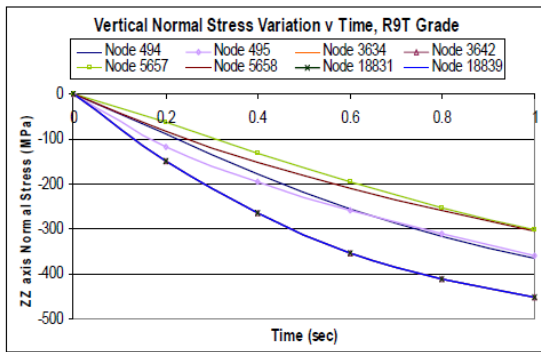Fig. 8 Variation of normal stresses in the rolling direction

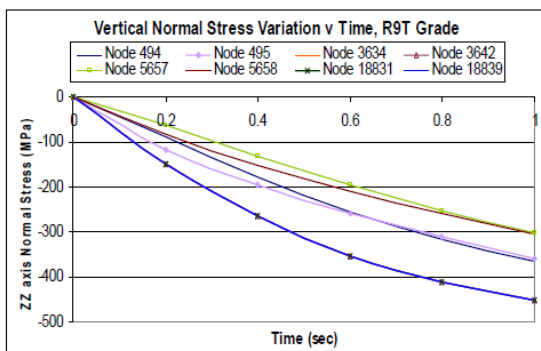Fig. 9 Variation of normal stresses in the vertical direction

Fig. 10 Variation of normal stresses in the lateral direction

The field of normal stresses (in the different directions) due to normal loading can be seen in Figs. 8 to 10. It is worth noting that the trend and to some extent magnitude of these stresses are similar. This subject indicates that the stress field within the wheel-rail interface is hydrostatic.

VII. CONCLUSION

In this stage of static failure analysis, it was found that the wheel was unlikely affected by high stress status, except in the normal loading within the minimum principle stress. The stress field within the interface leads to plastic deformation at the wheel material, and as a result, crack initiation phase had likely happened.

Maximum normal stress belongs to node 495, which is at the depth of 3mm subsurface. It is worth noting that all nodes with drawn normal stress are related to the engaged element with the rail. In other words, this element experiences utmost stresses.

The subsurface cracks might have propagated with high temperature created by composite brake shoes during the steepest gradient of the track. So, future work study could be preferably extended to the model in two following fields; (1) deploying a dynamic simulation package to find out the contact patch features and applied forces, and (2) investigating the effects of the braking process on the variation of the contact surface and subsurface.

Also, the remained items could complete the work study: (3) inclusions as a basis for crack initiation could be further investigated, and (4) Fatigue crack growth with respect to the life, the crack direction and critical fracture.

REFERENCES

[1] K. L. Johnson, *Contact Mechanics*, Cambridge University Press, 1985.
[2] UIC code 812-3 leaflet, *Technical specification for the supply of rough rolled non-alloy steel tyres for tractive and trailing stock*, 5th Ed, International Union of Railways, 1984.
[3] A. Fallah, A. Asadi Lari and S. A. Jazayeri, "Determination of the effective factors on the tractive effort of Diesel-Electric locomotives in Iranian Railway Network", *Proceedings of ISME2008*, Kerman, 2008 (in Persian).
[4] A. Kapoor, F. Schmid and D. Fletcher, "Managing the critical wheel/rail interface", *Railway Gazette International*, January 2002.
[5] A. Ekberg, "Rolling contact fatigue of railway wheels-towards tread life prediction through numerical modeling considering material imperfections", PhD thesis summary, Department of solid mechanics, Chalmers university of technology, 2000.
[6] A. Ekberg and P. Sotkovszki, "Anisotropy and rolling contact fatigue of railway wheels", *Int. J. Fatigue*, vol. 23, pp. 29-43, 2001.
[7] A. Ekberg and E. Kabo, "Fatigue of railway wheels 6 and rails under rolling contact and thermal loading – an overview", *Wear*, vol. 258, pp. 1288-1300, 2005.
[8] J. W. Ringsberg, "Shear mode growth of short surface-breaking of RCF cracks", *Wear*, vol. 258, pp. 955-963, 2005.
[9] M. Akama, "Development of Finite Element Model for Analysis of Rolling Contact Fatigue Cracks in wheel/rail systems", PhD Senior Researcher, Vehicle Strength, Vehicle Structure Technology Division.
[10] Y. Liu, B. Stratman and S. Mahadevan, "Fatigue crack initiation life prediction of railroad wheels", *Int. Journal of Fatigue*, vol. 28, pp. 747-756, 2006.